34th Annual International Conference of the IEEE EMBS
San Diego, California USA, 28 August - 1 September, 2012

Investigation of the role of crimps in collagen fibers in tendon with a microstructually based finite element model

Vickie Shim, Justin Fernandez, Thor Besier, and Peter Hunter

Abstract— **Tendon has a hierarchical structure that links tendon, fascicle, fibre and fibrils. In particular tendon fibres are made up of fibrils that have distinctive wavy forms called crimps. Experimental and imaging studies have shown that this crimp pattern plays an important role in mechanical properties of tendon but its exact influence has not been identified. We have developed a micro finite element model of tendon that contains accurate crimp patterns embedded in the model. This model utilizes a unique material coordinate system that is aligned in the direction of fibres. The crimp was implemented by performing fibre fitting procedure, which aligns the material coordinate system according to the crimp angle. FE analysis study was performed to identify the influence of crimp morphology on stress distribution pattern in tendon. Introduction of crimp angle to the model produced heterogeneous deformation and stress transfer patterns whereas the one without any crimp patterns predicted a uniform stress pattern. Future works include parametric studies on the influence of crimp pattern and morphology on stress distribution pattern in the tissue.**

I. Introduction

Tendon is a load bearing tissue that connects muscle to bone, which produces joint motion by transmitting tensile loads from muscle to bone[1]. The structure of tendon is characterized by a well-organized hierarchy within the tissue [2](Figure 1). Starting from collagen fibrils, the basic structural component of tendon that are packed within a matrix rich in proteoglycans, fibrils are formed into fibre, which in turn form fascicles. These fascicles are the major constituents of the whole tendon tissue.

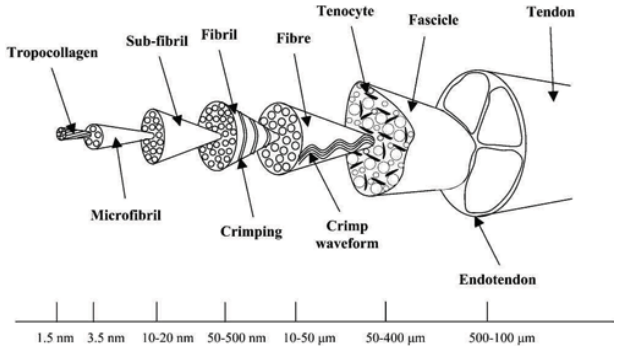

Figure 1. Hierarchical structure of tendon (from [1])

One important feature of the fibres in tendon is that they display gentle planar sinusoidal waviness, which is called the 'crimp' of collagen and mechanical properties of tendons are dependent on this unique arrangement and properties of collagen fibres. In fact, tensile tests of tendon performed along the collagen fibre axis display a characteristic nonlinear curve (Figure 2) where the upwardly concave region appears first as collagen crimp pattern is straightened followed by a linear region, which is dominated by material properties of straightened collagen[3]. However the effect of crimp patterns on mechanical behavior of tendon fibres has not been clearly described. Therefore the aim of this study is to develop a microstructurally based finite element (FE) model of tendon that can reproduce this characteristic structure-function relationship of tendon fibres in order to investigate the role crimps in tissue deformation and internal stress distribution patterns.

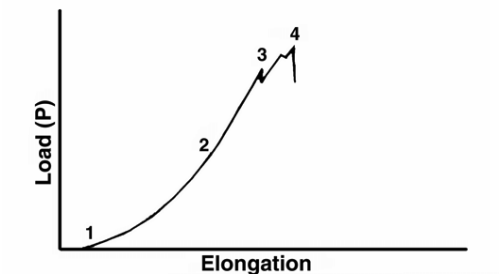

Figure 2: Load elongation curve of tendon fibre (from [1])

II. Materials and Methods

*Research supported by Australian Research Council Linkage Grant

Vickie Shim is with the Auckland Bioengineering Institute, University of Auckland, Auckland, New Zealand (phone: 64 3737599x86932; fax: 64 9 367 7157; e-mail: v.shim@auckland.ac.nz).

Justin Fernandez is with the Auckland Bioengineering Institute, University of Auckland (e-mail: j.fernandez@auckland.ac.nz).

Thor Besier is with the Auckland Bioengineering Institute, University of Auckland (e-mail: t.besier@auckland.ac.nz).

Peter Hunter is with the Auckland Bioengineering Institute, University of Auckland, New Zealand (e-mail:p.hunter@auckland.ac.nz)

A. Governing equation for finite element analysis

A micro finite element model of tendon fibre with crimp waveform was developed. The crimp was implemented by utilizing a microstructually based material coordinate system where the stresses and strains are referred to a material coordinate system rather than the original reference coordinate system. This is useful when describing a constitutive law, which refers to microstructural directions in tissue. In our model, the axes in the material coordinate system are aligned with the fibre direction in tendon. This new coordinate system ν_α, is related to the original rectangular Cartesian base vectors g_k covariant (a_α^υ) and contravariant (a_υ^α) base vectors shown below.

$$\mathbf{a}_\alpha^\nu = \frac{\partial x_k}{\partial \nu_\alpha}\mathbf{g}_k^x \quad \text{and} \quad \mathbf{a}_\nu^\alpha = \frac{\partial \nu_\alpha}{\partial x_k}\mathbf{g}_x^k.$$

Then tensors for stress and strain expressed in the rectangular Cartesian coordinate can be transformed to this microstructural coordinate system through covariant $a_{\alpha\beta}^{\upsilon}$ and contravariant metric tensors $a_\nu^{\alpha\beta}$ defined as the following.

$$a_{\alpha\beta}^\nu = \mathbf{a}_\alpha^\nu \cdot \mathbf{a}_\beta^\nu = \frac{\partial x_k}{\partial \nu_\alpha}\frac{\partial x_k}{\partial \nu_\beta} \text{ and } a_\nu^{\alpha\beta} = \mathbf{a}_\nu^\alpha \cdot \mathbf{a}_\nu^\beta = \frac{\partial \nu_\alpha}{\partial x_k}\frac{\partial \nu_\beta}{\partial x_k}.$$

The governing equation can be derived by considering conservation of linear and angular momentum as well as conservation of mass. Then the equation in weak form will become the following.

$$\int_{V_0^n} T^{\alpha\beta}F_\beta^j \frac{\partial \delta u_j}{\partial X_\alpha} \mathrm{dV}_0^n = \int_{S_c^n} \mathrm{f_c}\delta \mathrm{u_j^c} \mathrm{dS_c^n},$$

where S_c^n is the surface in contact at current configuration, $\delta\mu_j$ the virtual displacement field in the jth direction, V_0^n the undeformed volume, f_c contact force, φ_n^{3D} the 3D geometric basis function, F_β^j the deformation gradient, $T^{\alpha\beta}$ the 2nd Piola-Kirchoff stress tensor, which is expressed in microstructural coordinate system as the following

$$T^{\alpha\beta} = \frac{1}{2}\left(\frac{\partial \bar{W}}{\partial E_{\alpha\beta}} + \frac{\partial \bar{W}}{\partial E_{\beta\alpha}}\right) - pa_\nu^{\alpha\beta} + T_0 a_\nu^{11}\delta_1^\alpha\delta_1^\beta.$$

where W is a strain energy function, p is the hydrostatic pressure and $E_{\alpha\beta}$ is the Green strain tensor, which is given in a microstructural axis as the following

$$E_{\alpha\beta} = \frac{1}{2}\left(\frac{\partial x_k}{\partial \nu_\alpha}\frac{\partial x_k}{\partial \nu_\beta} - \frac{\partial X_k}{\partial \nu_\alpha}\frac{\partial X_k}{\partial \nu_\beta}\right) = \frac{1}{2}\left(a_{\alpha\beta}^\nu - A_{\alpha\beta}^\nu\right),$$

More detailed treatment of the derivation of governing equation in microstructurally based coordinate system can be found in [4]

B. Constitutive laws

Material behaviour of tendons is relatively insensitive to strain rate. Moreover once preconditioned, minimum amount of hysteresis occurs, indicating that time and rate dependent components may be removed in capturing the macroscopic material behaviour. Therefore we used the incompressible, transversely isotropic hyperelasticty in our material description, which is structurally motivated representation of tissue behaviour[2]. The strain energy function has the following form.

$$W = W_1(I_\mathbf{C}, II_\mathbf{C}) + W_2(\lambda_{\text{fiber}}).$$

where W_1 represents the behaviour of ground substance and is described as a Moony-Rivlin material. W_2, on the other hand, describes the behaviour of crimped collagen fibre in tension. The expression for W_1 and W2 are given in the following where I_c, II_c are isotropic invariants of deformation tensor C.

$$W_1 = \frac{C_1}{2}(I_C - 3) + \frac{C_2}{2}(II_C - 3).$$

$$\lambda_{\text{fiber}}\frac{\partial W_2}{\partial \lambda_{\text{fiber}}} = 0, \text{ for } \lambda_{\text{fiber}} < 1,$$

$$\lambda_{\text{fiber}}\frac{\partial W_2}{\partial \lambda_{\text{fiber}}} = C_3[e^{C_4(\lambda_{\text{fiber}}-1)} - 1], \text{ for } 1 < \lambda_{\text{fiber}} < \lambda^*_{\text{fiber}}, \text{ and}$$

$$\lambda_{\text{fiber}}\frac{\partial W_2}{\partial \lambda_{\text{fiber}}} = C_5\lambda_{\text{fiber}} + C_6, \text{ for } \lambda \geq \lambda^*_{\text{fiber}},$$

W_2 is a piecewise function that describes different regions in the load strain curve of tendon. λ_{fiber} is fibre stretch ratio and λ^*_{fiber} depicts the point in fibre stretch ratio where the fibre is completely stretched (end point of the toe region 1 in Figure 2). The seven parameters for this constitutive relationship were obtained from Pena et al. [5]who found the values for these parameters for the patella tendon (PT). They performed material property optimization based on the experimental data [6].These values are given in the following table.

	C1	C2	C3	C4	C5	λ*
PT	2.75	0.0	0.065	115.89	777.56	1.042

Table1: Parameter values used in the model.

C. Fibre fitting procedure

Since the fibres in tendon have the unique waviness called crimp, the fibre direction in the microstructural coordinate system was modified to capture this crimp pattern. Specifically we employed the fibre fitting procedure [7]. Depending on the prescribed crimp angle, a data set was generated that captured the crimp angle in a sinusoid waveform. Then the vectors that describe the directions in the crimp wave were generated from the data set, which were than turned into direction cosines in the original rectangular Cartesian coordinate system. Then three Euler

angles of those vectors in the material coordinate were obtained. The result of fibre fitting is shown below (Figure 3). Using this technique, we can describe any crimp angle

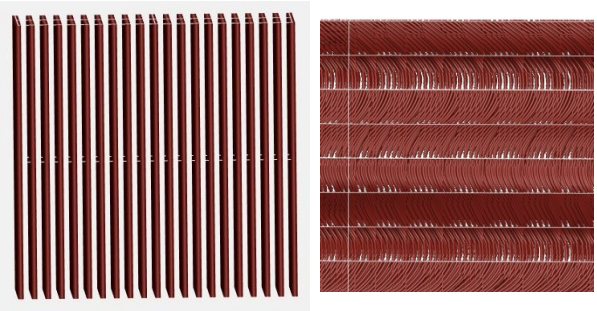

(a) Before fitting (b) After fitting

Figure 3. Result of Fibre fitting. A wavy crimp pattern was introduced after the fitting

Two models were generated – one with no crimp angle and another with a crimp angle of 30°. Each model had 8 3D elements. We also used high order cubic Hermite basis function, which enabled us to describe tissue geometry with a relatively small number of elements. These two models were then run with the same boundary condition, which applied uniaxial tension up to 10% in steps of 1% while fixing the bottom four nodes completely. In doing so, a stress/strain curve for both cases was obtained and compared in order to investigate the influence of crimp angles on stress distribution pattern. A specialized FE software called CMISS (www.cmiss.org, freely available for academic use) was used in FE analysis as well as in the fibre fitting process.

III. Results

Our model was able to generate the characteristic stress strain curve of tendon. When compared with the experimental data in the literature, the predicted stress-strain curve followed closely the experimental curve reported by Butler et al.[6] as seen in Figure 4.

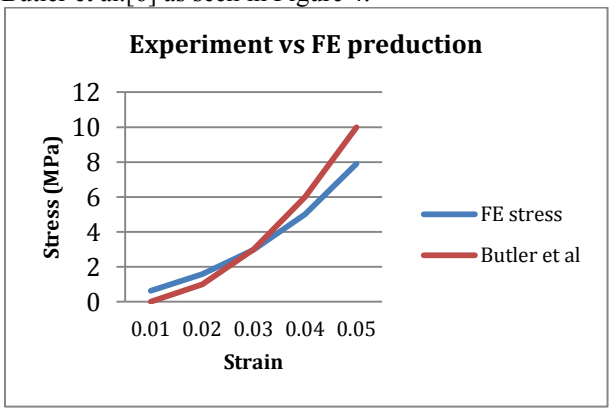

Figure 4. Comparison of experimental results and FE predictions in terms of stress vs. strain curve

Then the deformation and stress pattern of FE models with and without crimp pattern were compared. Firstly the model with crimp angle exhibited wavy deformation pattern whereas the model with no crimp angle exhibited straight deformation as shown in the following figure.

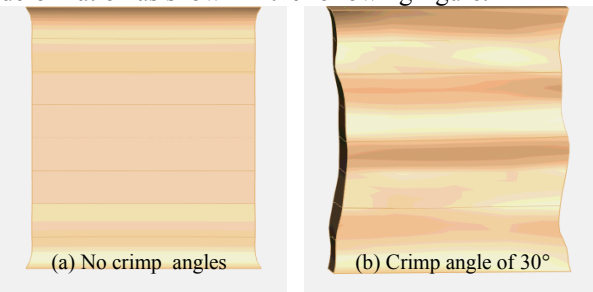

Figure 5: Tissue deformation pattern for models with and without crimp pattern

In terms of stress pattern, these two models showed different von Mises stress distribution patterns as shown below.

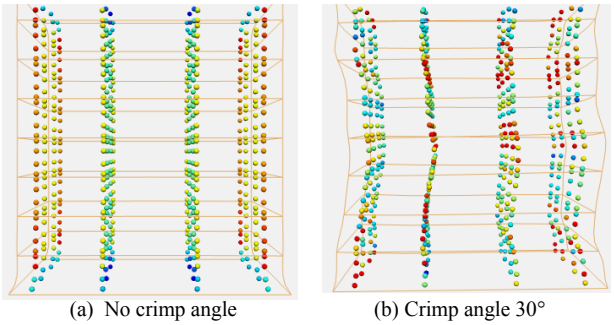

(a) No crimp angle (b) Crimp angle 30°

Figure 6. Internal stresses (von Mises) for models with and without crimp patterns

As can be seen above, tissue with crimp angle produced inhomogeneous internal stress pattern (according to the crimp patterns in the fibre) whereas the one with no crimp angle showed rather homogenous internal stress pattern.

The stress-strain curves for these two cases were compared as well in Figure 7.

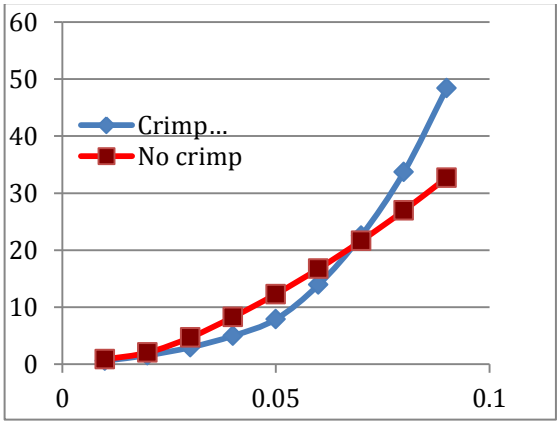

Figure 7. Stress-strain curve for strains up to 10% for models with and without crimp patterns.

As can be seen, the crimp pattern introduced upward concave shape of a toe region in the stress-strain curve whereas the model without any crimp failed to display this shape.

IV. CONCLUSIONS

We have developed a microstructurally based finite element model of tendon. In this model, the characteristic crimp angle was embedded using the material coordinate system in our FE model. Specifically we have aligned the material coordinate system according to the prescribed crimp angle by performing the fibre fitting procedure. The resulting model was able to generate the characteristic J shape curve usually shown in tendon unaxial tensile experiment. In particular the predicted values from our model closely matched experimental values reported in the literature.

The toe region of the curve was due to crimp patterns in collagen fibres as the model without crimp failed to show this characteristic non-linear curve. Moreover the tissue deformation and internal stress pattern for the model with crimp patterns were different from the one without crimp patterns in the fibre. Specifically, the inhomogeneous stress and deformation pattern shown in the model with a crimp angle followed closely the crimp pattern embedded in the model, indicating the significant impact that crimp pattern has on the micromechanical tissue deformation and stress distribution.

The strength of our model is that we can prescribe any crimp angles to the model, including helical angle. Moreover we can also assign heterogeneous crimp patterns to a finite element model in the same manner as assigning location dependent material properties. Therefore if tissue images with detailed crimp pattern are available, these can be used to create microstructally based finite element models of tendon. These models can be used in various parametric studies by systematically varying tissue microstructural properties. Such model will have potential to shed light on elucidating the onset and progress of tendinopathy.

ACKNOWLEDGMENT

This work was supported by the Australian Research Council Linkage grant on Bioengineered Bioscaffolds for Achilles Tendinopathy Treatment (LP110100581)

REFERENCES

[1] S. Cowin, and S. Doty, *Tissue Mechanics*, New York, USA: Springer, 2006.

[2] J. A. Weiss, and J. C. Gardiner, "Computational modeling of ligament mechanics," *Crit Rev Biomed Eng,* vol. 29, no. 3, pp. 303-71, 2001.

[3] R. Grytz, and G. Meschke, "Constitutive modeling of crimped collagen fibrils in soft tissues," *J Mech Behav Biomed Mater,* vol. 2, no. 5, pp. 522-33, Oct, 2009.

[4] J. W. Fernandez, and P. J. Hunter, "An anatomically based patient-specific finite element model of patella articulation: towards a diagnostic tool," *Biomech Model Mechanobiol,* vol. 4, no. 1, pp. 20-38, Aug, 2005.

[5] E. Pena, B. Calvo, M. A. Martinez *et al.*, "Effect of the size and location of osteochondral defects in degenerative arthritis. A finite element simulation," *Comput Biol Med,* vol. 37, no. 3, pp. 376-87, Mar, 2007.

[6] D. L. Butler, M. Y. Sheh, D. C. Stouffer *et al.*, "Surface strain variation in human patellar tendon and knee cruciate ligaments," *J Biomech Eng,* vol. 112, no. 1, pp. 38-45, Feb, 1990.

[7] I. J. Legrice, P. J. Hunter, and B. H. Smaill, "Laminar structure of the heart: a mathematical model," *Am J Physiol,* vol. 272, no. 5 Pt 2, pp. H2466-76, May, 1997